Received: 15 May 2019 | Revised: 7 November 2019 | Accepted: 19 November 2019

DOI: 10.1002/eco.2175

RESEARCH ARTICLE

WILEY

A global-scale analysis of water storage dynamics of inland wetlands: Quantifying the impacts of human water use and man-made reservoirs as well as the unavoidable and avoidable impacts of climate change

Petra Döll[1,2] | Tim Trautmann[1] | Mareike Göllner[1] | Hannes Müller Schmied[1,2]

[1] Institute of Physical Geography, Goethe University Frankfurt, Frankfurt am Main, Germany

[2] Senckenberg Leibniz Biodiversity and Climate Research Centre Frankfurt (SBiK-F), Frankfurt am Main, Germany

Correspondence
Petra Döll, Institute of Physical Geography, Goethe University Frankfurt, Frankfurt am Main, Germany.
Email: p.doell@em.uni-frankfurt.de

Abstract

Wetlands such as bogs, swamps, or freshwater marshes are hotspots of biodiversity. For 5.1 million km^2 of inland wetlands, the dynamics of area and water storage, which strongly impact biodiversity and ecosystem services, were simulated using the global hydrological model WaterGAP. For the first time, the impacts of both human water use and man-made reservoirs (WUR) and future climate change (CC) on wetlands around the globe were quantified. WUR impacts are concentrated in arid/semiarid regions, where WUR decreased mean wetland water storage by more than 5% on 8.2% of the mean wetland area during 1986–2005 (A_m), with highest decreases in groundwater depletion area. Using output of three climate models, CC impacts on wetlands were quantified, distinguishing unavoidable impacts [i.e., at 2 °C global warming (GW)] from avoidable impacts (difference between 3 °C and 2 °C impacts). Even unavoidable CC impacts are projected to be much larger than WUR impacts, also in arid/semiarid regions. On most wetland area with reliable estimates, avoidable CC impacts are more than twice as large as unavoidable impacts. In case of 2 °C GW, half of A_m is estimated to be unaffected by mean storage changes of more than 5%, but only one third in case of 3 °C GW. Temporal variability of water storage will increase for most wetlands. Wetlands in dry regions will be affected the most, particularly by water storage decreases in the dry season. Different from wealthier countries, low-income countries will dominantly suffer from a decrease in wetland water storage due to CC.

KEYWORDS

climate change, water storage, water use, wetland, reservoirs, global

This is an open access article under the terms of the Creative Commons Attribution License, which permits use, distribution and reproduction in any medium, provided the original work is properly cited.
© 2019 The Authors. Ecohydrology published by John Wiley & Sons Ltd

1 | INTRODUCTION

It is difficult to clearly define the term wetland, which is related to the fact that wetlands are transitional between terrestrial and aquatic systems, and multiple definitions are in use (Lehner & Döll, 2004; Sharitz, Batzer, & Pennings, 2014). "For ecologists seeking a biologically useful definition of wetland," Sharitz et al. (2014, p. 2) suggested the definition of Keddy (2000): "A wetland is an ecosystem that arises when inundation by water produces soils dominated by anaerobic processes and forces the biota, particularly rooted plants, to exhibit adaptations to tolerate flooding. "The U.S. Army Corps of Engineers, the primary permitting agency for wetlands of the United States, provided a definition that is more specific with respect to hydrological processes (Environmental Laboratory, 1987, cited in Sharitz et al., 2014, p. 1): "The term 'wetlands' means those area that are inundated or saturated by surface or ground water at a frequency and duration sufficient to support, and that under normal circumstances do support, a prevalence of vegetation typically adapted for life in saturated soil conditions. Wetlands generally include swamps, marshes, bogs, and similar area."

Compared with the areal fraction of wetlands on the Earth's land surface, wetlands offer disproportionally high ecosystem services as they are the habitat of a high number of animal and plant species, and they improve water quality and mitigate floods (Sharitz et al., 2014). Wetlands account for about 30% of global emissions of the greenhouse gas methane (IPCC, 2013). Most wetlands are carbon and radiative sinks (Mitsch et al., 2013). Thus, wetlands are important for human well-being and play a major role in the two problem fields that threaten sustainable development of the Earth system the most, biodiversity loss and climate change (CC). Regarding CC, wetland dynamics are of interest for both assessing potential ecological impacts and greenhouse gas emissions. Unfortunately, human activities including construction of dykes for flood protection, land drainage for food production and infrastructure construction as well as water abstractions have led to a significant degradation and loss of wetlands (Finlayson et al., 2005; Junk et al., 2013). CC puts additional stress on wetlands and may lead to further wetland loss in some regions, in particular in currently dry regions (Döll et al., 2015; Settele et al., 2014).

The IPCC (2014) concluded with medium confidence that within this century, magnitudes and rates of CC associated with medium- to high-emission scenarios [Representative Concentration Pathway (RCP)4.5, RCP6.0, and RCP8.5] pose a high risk of abrupt and irreversible regional-scale change in the composition, structure, and function of ecosystems, including wetlands. CC alters ecologically relevant characteristics of streamflow regimes and wetland water dynamics, which affect, together with CO_2-enrichment and temperature rise, habitat quality and food webs (Döll & Bunn, 2014; Settele et al., 2014). For example, unless precipitation is increasing, increasing temperature interannual variability will most likely decrease water storage and flow during the low-flow season, leading to reduced water quality in remnant pools, reduction in floodplain egg and seed banks and loss of permanent aquatic refugia for fully aquatic species and water birds (Settele et al., 2014). However, although there are general qualitative assessments of CC impacts on wetlands and their ecosystem services, geographically explicit projections of CC impacts on wetland water storage are missing at continental and global scales (Brander et al., 2012; Twilley & Brinson, 2014). The study of Schneider, Flörke, de Stefano, and Petersen-Perlman (2017) was restricted to CC impact on overbank flow into riparian wetlands at 93 Ramsar sites ("wetlands of international importance," www.ramsar.org) around the globe, but also quantified the impact of present-day water use and man-made reservoirs (WUR). Schneider et al. (2017) found the WUR had decreased overbank flow volume by more than 30% as compared with natural conditions at 37% of all sites, whereas CC was projected to lead to such decreases (until the 2050s under the greenhouse gas emissions scenario RCP6.0) at 16% and to such increases at 30% of the investigated Ramsar sites.

With their Global Lakes and Wetland Database (GLWD), Lehner and Döll (2004) provided the location of different types of wetlands as well as of lakes and man-made reservoirs on the Earth's continents by compiling information from a number of data sources, mainly maps. They found that wetlands cover 9 ± 1 million km^2 (6.2–7.6% of global land surface excluding Antarctica and Greenland). It is difficult to judge the accuracy of this data set. Maps tend to show the maximum extent of temporally variable inundation area, and the widespread loss of wetlands over the past century might not be reflected in maps and therefore in GLWD. Most other data sets show a smaller global extent of wetlands (Davidson, Fluet-Chouinard, & Finlayson, 2018; Lehner & Döll, 2004; Mitsch et al., 2013). Still, there are more recent estimates with larger global wetland extents (Davidson et al., 2018; Tootchi, Jost, & Ducharne, 2019). However, due to numerous difficulties in detecting wetlands by remote sensing, including the distinction from lakes (Papa et al., 2010; Pekel, Cottam, Gorelick, & Belward, 2016; Schroeder et al., 2015), and the lack of high quality national inventories, there is not yet a more reliable global wetlands data set (see also Section 4). Simulating the occurrence of wetlands (including their dynamical extents) by hydrological modelling (e.g., Stacke & Hagemann, 2012) could help characterizing wetlands under natural conditions, but results are very uncertain.

Information on wetland degradation is even more uncertain (Finlayson et al., 2005). Based on 189 reports on wetland area change at local to global scales, Davidson (2014) concluded that up to 70% of wetlands existing in 1900 had been lost by the beginning of the 21st century. Percent losses of inland wetlands were roughly estimated to be highest in Asia and the Neotropics (Caribbean, Central, and South America) and lowest in North America. Losses continue to happen in all parts of the world, with the highest rates in Asia, in spite of the Ramsar Convention (Davidson, 2014).

Although wetland inventories are paramount, they do not inform about temporal dynamics. The concept of a "hydropattern" was established by wetland ecologists to describe the temporal variations of wetland water storage, wetted, or inundation area as well water table elevations that are important for the ecology of wetlands and the well-

being of wetland biota (Jackson, Thompson, & Kolka, 2014). According to Mendelssohn et al. (2014, p. 61), wetland animals are generally more affected by drying constraints and plants more by flooding constraints. Although hydropatterns during recent decades can be derived, to a certain extent, from remote sensing, projections of future wetland area and water storage can only be achieved by hydrological modelling. Equally, hydrological modelling can contribute to assessing the impact of human activities on wetland dynamics, in particular the impacts of water abstractions and man-made reservoirs.

The objective of this paper is to provide a global-scale analysis of wetland water dynamics, based on simulations with a global hydrological model. In the first part of the paper, the current (1986–2005) situation of water storage dynamics in inland wetlands and derived variations in wetland extent is shown, and the impacts of human WURs on natural wetland water storage dynamics are estimated. In the second part, we quantify both unavoidable and avoidable CC impacts on wetland water storage dynamics until the end of the 21st century, taking into account the uncertainty of global climate model output. Although impacts occurring in case of a 2 °C global warming (GW) appear to be unavoidable, a 3 °C GW can still be avoided by climate mitigation, and the difference in potential impacts under the two GW levels can be regarded as the avoidable CC impact.

In Section 2, we describe (a) how the global water resources and use model WaterGAP (Müller Schmied et al., 2014) simulates wetland storage and area based on wetland information from GLWD and (b) the applied climate data, indicators and methods for determining the reliability of the simulations. Section 3 shows the current situation of global wetlands and WUR impacts as well as projected changes in wetland water storage dynamics including the quantification of avoidable impacts. In Section 4, we discuss various uncertainties as well as implications of the results for CC mitigation and adaptation. Finally, we draw conclusions in Section 5.

2 | METHODS AND DATA

2.1 | The global water resources and use model WaterGAP

2.2 | Overview

With a spatial resolution of 0.5° latitude by 0.5° longitude (55 km by 55 km at the equator), the global water resources and use model WaterGAP computes both water resources, that is, water flows and storages, and human water use on all land area of the globe except Antarctica. Water withdrawals and consumptive water use in the sectors households, manufacturing, cooling of thermal power plants, livestock, and irrigation are computed by five water use models. Then, net water abstractions from groundwater and surface water, the difference between withdrawals and return flows, are computed in the linking model GWSWUSE and become input of the WaterGAP Global Hydrology Model (WGHM), together with time series of climate variables (Müller Schmied et al., 2014). WGHM computes various water

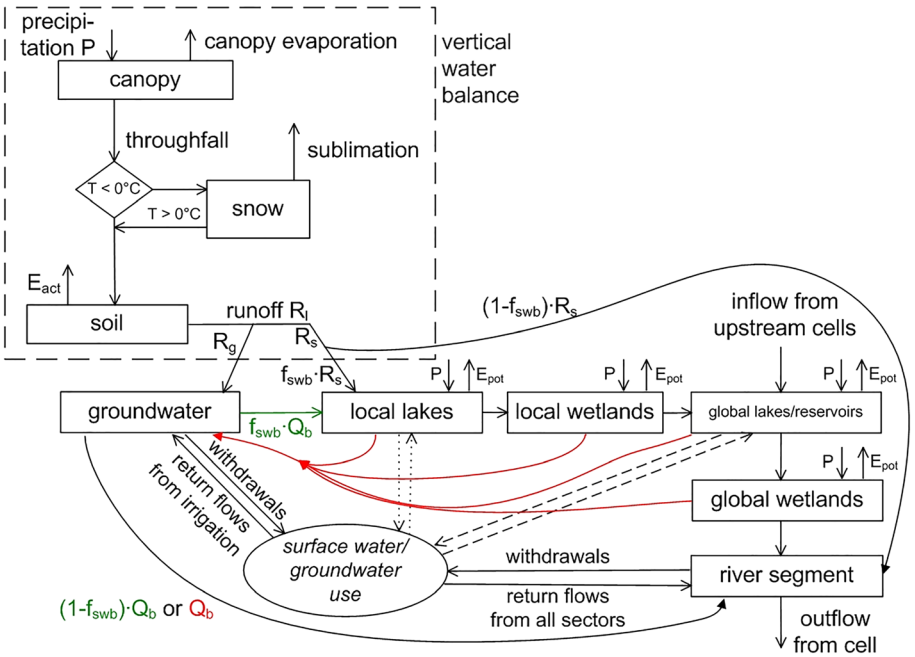

FIGURE 1 Schematic of water storage compartments (boxes) and flows (arrows) within each 0.5° grid cell of the WaterGAP Global Hydrology Model (WGHM), including the simulation of impacts of man-made reservoirs and human water use on water storages and flows. Depending on the areal fraction of surface water bodies in the grid cell f_{swb}, a part of surface runoff and of the groundwater outflow is routed through lakes and wetlands before reaching the river. In arid/semiarid regions, lakes and wetlands lose water to the groundwater, whereas in humid areas, groundwater recharges lakes and wetlands. Global lake and global reservoir storages are calculated separately. Flows that are only simulated in arid/semiarid regions are shown in red and those occurring only in humid regions are shown in green. (Figure from Döll, Müller Schmied, Schuh, Portmann, & Eicker, 2014)

flows (e.g., evapotranspiration, groundwater recharge, and streamflow, see Figure 1) as well as water storage in 10 compartments, including snow, soil, groundwater, and the surface water bodies lakes, man-made reservoirs, wetlands, and rivers (boxes in Figure 1).

WGHM is calibrated against observed mean annual streamflow by adjusting one to three parameters in the upstream area of the station (Müller Schmied et al., 2014). Using a regression equation, one parameter is then regionalized to the ungauged area of the globe. In the WaterGAP 2.2b version applied in this study, calibration was done for 1,319 streamflow gauging stations. Due to this calibration, WaterGAP very often shows a better performance with respect to observed streamflow than other global hydrological models (Döll, Douville, Güntner, Müller Schmied, & Wada, 2016; Gudmundsson et al., 2012; Tallaksen & Stahl, 2014; Veldkamp et al., 2018; Zaherpour et al., 2018). Still, for many rivers WaterGAP cannot appropriately simulate streamflow seasonality and other streamflow regime characteristics, in particular when streamflow is strongly affected by human interference (Hunger & Döll, 2008). WaterGAP 2.2b Nash-Sutcliffe efficiencies for monthly streamflow at the 1,319 gauging stations are larger than 0.7 for 372 stations, between 0.5 and 0.7 for 349 station and smaller than 0.5 for 598 stations.

2.2.1 | Simulation of wetland water storage dynamics in WGHM

The model distinguishes so-called "global" wetlands, that is, catchment-fed wetlands, from "local" wetlands, that is, locally-fed wetlands, and takes into account the areal fraction of both wetland categories in each 0.5° grid cell. While local wetlands only obtain water from the runoff generated within a grid cell, in addition to precipitation onto the wetland area, global wetlands receive also inflow from the upstream grid cell(s) (Figure 1). The dynamic water balance of the local and the global wetland in a cell is computed separately as

$$\frac{dS_w}{dt} = Q_{in} + A(P - PET - R_{gw}) - Q_{out}, \quad (1)$$

with S_w: volume of water stored in the (local or global) wetland (cubic metres), t: time (day), Q_{in}: inflow into wetland (cubic metres per day), A: (global or local) wetland area in grid cell (square metres), P: precipitation (metres per day), PET: potential evapotranspiration (metres per day), R_{gw}: groundwater recharge from wetland (only in arid/semiarid regions (metres per day), Q_{out}: outflow from wetland to other surface water bodies (cubic metres per day; see Figure 1). In case of local wetlands, Q_{in} includes inflow from groundwater, a fraction of the groundwater recharge in the cell, and inflow from a fraction of the fast surface and subsurface runoff of the cell; in both cases, the fraction depends on the fraction of surface water area in the cell f_{swb} (Figure 1). In case of global wetlands, there is an additional inflow from the upstream streamflow even in the low-flow season.

To simulate the temporally varying wetland area, it is calculated in each daily time step as a function of wetland water storage, with

$$A = r\,A_{max} \quad (2)$$

$$r = 1 - \left(\frac{|S_w - S_{wmax}|}{S_{wmax}}\right)^p, \quad (3)$$

with r: reduction factor (−), A_{max}: maximum extent of all global (or local) wetlands in grid cell (square metres), S_{wmax}: maximum volume of water that can be stored in wetland (cubic meters), and p = 3.32. S_{wmax} is set to A_{max} x 2 m; any excess water becomes outflow. According to Equation (3), wetland area is reduced by 10% if wetland water storage is only 50% of the maximum. Outflow from wetlands is simulated as a function of wetland water storage. In case of global wetlands, Q_{out} is assumed to be equal to kS_w, with k = 0.01/d, whereas outflow from local wetlands is assumed to be slower and is simulated by multiplying kS_w with $(S_w/S_{wmax})^{2.5}$. The dynamics of floodplain inundation due to overbank flow is not simulated in WGHM.

2.2.2 | Simulated and evaluated wetlands

In WaterGAP, location and area of wetlands as provided by the Global Lakes and Wetlands Dataset (GLWD, Lehner & Döll, 2004) are taken into account. The subset GLWD-3 represents lakes, man-made reservoirs, rivers, and different wetland classes in the form of a global raster map at 30-arcs resolution (derived from various polygon data sets). Wetlands classes are (a) freshwater marsh/floodplain, (b) swamp forest/flooded forest, (c) coastal wetland, (d) pan/brackish/saline wetland, (e) bog/fen/mire, (f) intermittent wetland/lake, (g) 50–100% wetland, (h), 25–50% wetland and (i) wetland complex (0–25%). GLWD-3 provides approximately the temporal maximum of wetland extent as wetland outlines were mainly derived from maps and is used to determine A_{max}. In case of various input data sets, a wetland was assumed to be present if at least one of the data sets showed one. Lakes and reservoirs of GLWD-3 are explicitly simulated as lakes and reservoirs in WGHM (Figure 1) whereas wetland classes "coastal wetland" (covering 660,000 km^2) and "intermittent wetland/lake" (690,000 km^2) are not included in WGHM. Inclusion of coastal wetlands would require the simulation of ocean–land interaction, whereas intermittent wetlands/lakes of GLWD-3 cover very large parts of the deserts (cf. Figure 5 in Lehner & Döll, 2004) that cannot be assumed to be covered totally by water at any time but rather represent area where very rarely and at different points in time some parts may be flooded. Rivers shown in GLWD-3 are considered to be (lotic) wetlands and are included as wetlands in WGHM. It is assumed that only a river with adjacent wetlands (floodplain) is wide enough to appear as a polygon on the coarse-scale source maps (Lehner & Döll, 2004). For the fractional wetland type "50–100% wetland" (Figure 2), an arbitrary value of 75% grid cell coverage with wetland is assumed, for "25–50% wetland" a value of 35%, and for "wetland complex" a value of 15%. The large floodplain wetland of the lower Ganges–Brahmaputra in GLWD-3, covering almost all of Bangladesh, is not simulated as a wetland in WaterGAP, as during most of the time, only a small part of Bangladesh is inundated.

All wetlands subsumed in fractional classes are assumed to be local, that is, locally-fed. In case of all other wetland types, global

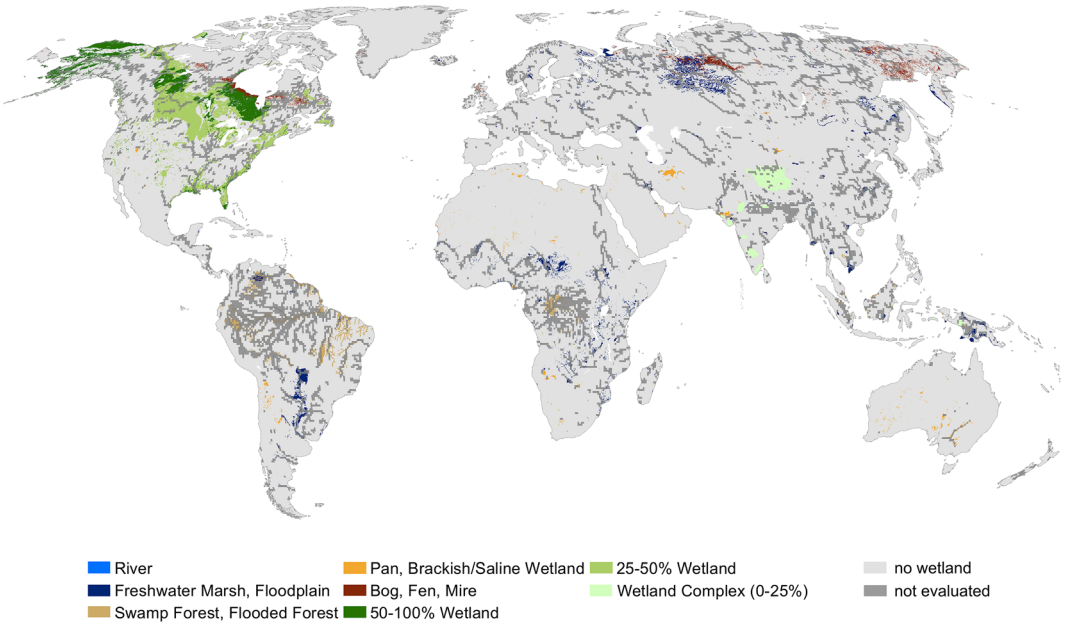

FIGURE 2 Wetlands according to the Global Lakes and Wetlands Database (Lehner & Döll, 2004) considered in WaterGAP simulations. Grid cells that could not be reliably evaluated with respect to wetland storage dynamics in this study are shown in dark grey

wetlands fed by the whole catchment were identified as follows. All wetland polygons with a direct connection to a major river (as defined by the big_river.shp file available from ESRI) are assumed to receive inflow from a large upstream area and are therefore categorized as global. However, if rivers in this file are categorized as intermittent, the adjacent wetlands are categorized as local in WaterGAP. All other wetlands are first buffered (to the inside, using a Geographic Information System) by a 10-km-wide ring such that the outer 10 km of a wetland are considered to be local and the core wetland area inside this buffer ring is considered to be global. The GLWD-3 area of all local and global wetlands of all types within in each 0.5° grid are finally summed to obtain the grid cell fractions of local and global wetlands (used to determine A_{max} in Equation 2).

Figure 2 shows the polygons of GLWD wetlands that are considered in WaterGAP simulations. The global sum of the maximum wetland area is 7.495 million km^2. For the evaluation of wetland water storage dynamics in this study, however, the 0.5° grid cells shown in dark grey could not be taken into account, which include 31.7% of the maximum wetland area in WaterGAP. Due to WaterGAP parameter choice and model algorithms, the simulated wetland water storage dynamics in these grid cells are deemed to be unreliable. The maximum water table variation in wetlands of 2 m that is assumed in WaterGAP as an appropriate value for most wetlands around the world is too small in tropical basins such that water storage in those wetlands is always at its maximum, whereas in reality there are temporal variations of the water tables. This occurs if inflow into the wetland is large as compared with the (underestimated) maximum storage volume, for example in most wetland cells in the Amazon basin where water tables are known to vary by up to 10 m (Fan & Miguez-Macho, 2011). Therefore, grid cells were excluded from further analysis if the wetland water table was during the reference period almost always very close to its maximum value of 2 m (i.e., if mean water table always >1.99 m for any of the climate data sets). Given our scarce knowledge about wetlands and their morphology at the global scale, it is currently not possible to derive a more precise global distribution of storage capacity. In addition, we excluded all "river" wetlands from the analysis because WaterGAP does not simulate inundation of floodplains due to overbank flow. Being global wetlands, river wetlands receive the total streamflow as inflow in WaterGAP (Figure 1) whereas in reality only the part of the streamflow that does not fit in the river channel flows into the floodplain. It would, however, not have been appropriate to exclude all these wetlands from the WaterGAP simulations as their inclusion does lead to an improved estimation of evaporation.

If wetland dynamics are incorrectly simulated in a cell, then the global wetlands in all downstream cells are not well simulated either. Therefore, downstream grid cells in which the global wetland area is larger than 10% of the total wetland area were also excluded from the evaluation. Out of 3.752 million km^2 of global and 3.743 million km^2 of local wetlands in WaterGAP, only 1.935 million km^2 of global and 3.184 million km^2 of local wetlands were included in our study. In total, the dynamics of 5.118 million km^2 of inland wetlands were evaluated, which amounts to 68.3% of the maximum wetland area considered in WaterGAP and 3.8% of the global land area (excluding Antarctica and Greenland). Unfortunately, most of the important wetlands in the Amazon, Congo, and Niger basins had to be excluded from the evaluation of wetland extent and storage dynamics (Figure 2).

2.2.3 | Simulating WUR impact on wetland storage

WGHM simulates the impact of WUR on waters storages and flows (Figure 1). Alternatively, WGHM can be applied to simulate water storages and flows that would occur if there were no WUR

(naturalized run). Net abstractions from surface water are taken from global lakes and reservoirs (first priority), rivers (second priority), and local lakes (third priority) but not directly from wetlands. However, they decrease wetland storage in the cell itself or the downstream cells by decreasing wetland inflows (Figure 1). Net abstractions from surface water may be negative, that is, water is added to the river, in case of significant groundwater abstractions with return flow to surface water bodies (see Figure 1 in Döll, Fritsche, Eicker, & Müller Schmied, 2014). Then, inflow into wetlands tends to increase due to human water use. In WGHM, net abstractions from groundwater decrease wetland water storage by decreasing groundwater outflow to surface water bodies including wetlands in the cell in which the abstractions takes place and by thus decreasing inflow to wetlands downstream (Figure 1). The opposite is true in case of negative net abstractions from groundwater, that is, man-made groundwater recharge due to irrigation with surface water. In naturalized runs, all net abstractions are set to zero.

Man-made reservoirs lead to increased evapotranspiration and thus decreased inflow into downstream global wetlands, and tend to decrease the seasonality of streamflow and thus of inflow to downstream wetlands. A total of 6,522 man-made reservoirs and 85 regulated lakes (lakes whose outflow is regulated by a dam) as provided by the Global Reservoir and Dam database (Lehner et al., 2011) are included in WaterGAP 2.2b. All identified regulated lakes have an area $\geq$100 km^2 and are global, with inflow from the upstream cell. The largest 1,026 reservoirs with a storage capacity $\geq$0.5 km^3 are classified as global, too. The water balance of all global lakes and reservoirs, which may cover more than one 0.5° grid cell, are computed in the respective outflow cells. If in rare cases, more than one reservoir has its outflow in the same grid cell, the reservoirs are aggregated. Consequently, the dynamics of 1,109 global reservoirs and regulated lakes are simulated by a specific reservoir algorithm that depends on whether their main purpose is irrigation or something else (Döll, Fiedler, & Zhang, 2009). The smaller reservoirs are treated as natural local lakes as the required lumping of all local reservoirs within a grid cell into one local reservoir per cell necessarily leads to a "blurring" of the specific reservoir characteristics, such that for local reservoirs, the reservoir algorithm is not expected to simulate water storage and fluxes better than the lake algorithm (Döll et al., 2009). In naturalized runs, the global reservoirs are assumed to be nonexistent, and the regulated lakes are simulated like natural lakes, whereas the smaller reservoirs are still treated like natural lakes. Therefore, when analysing the impact of man-made reservoirs on wetlands by comparing naturalized to standard runs of WGHM, only the impact of the largest 1,026 reservoirs and of 85 regulated lakes is determined.

2.3 | Climate data

WaterGAP2.2b was calibrated using the homogenized WFD_WFDEI daily climate data set. This 0.5° × 0.5° gridded data set of daily climate variables is based on ERA40 (WFD) and ERA-Interim (WFDEI, from 1979 onward) reanalysis data and was bias-corrected using a number of observational data sets (Weedon et al., 2014) and then homogenized (Müller Schmied et al., 2016). Observations include monthly values of precipitation provided by the Global Precipitation Climatology Centre, number of wet days, temperature, and cloud cover (Müller Schmied et al., 2016). In addition, monthly precipitation was corrected for a wind-induced undercatch (Weedon et al., 2014). This data set then served as input to WaterGAP for the analysis of the global wetland system during the reference period 1986–2005.

To analyse the impact of CC on wetland storage, WaterGAP 2.2b was driven for the time period 1979–2099 by the bias-corrected output of three CMIP5 global climate models (GCMs IPSL-CM5A-LR, GFDL-ESM 2M, and MIROC5) that were made available, with a spatial resolution of 0.5° × 0.5°, in the framework of the ISIMIP2b initiative (Frieler et al., 2017). For each GCM, both the low-emissions scenario RCP2.6 results and the higher-emissions scenario RCP6.0 results were provided. While the equilibrium climate sensitivity of IPSL-CM5A-LR is at the upper end of all CMIP models, the other two GCMs are at the lower end (Lange, 2017). For RCP6.0, global mean temperature (GMT) at the end of the 21st century is projected to be 3.5 °C above the preindustrial level by IPSL-CM5A-LR, whereas the other two GCMs project a GW of approximately 2.5 °C (Frieler et al., 2017). The corresponding values for RCP2.6 are 2.5 °C and 1.5 °C. However, the three GCMs do not span the range of regional climatic changes projected by the entire CMIP5 ensemble. To achieve that GCM output for historical periods is similar to observations, GCM output was bias-adjusted using the EWEMBI climate data set for 1979–2013, which is very similar to WFDEI over land (Lange, 2017). To isolate CC impacts, nonirrigation water use, irrigated area, reservoirs, and land use were kept at the level of 2005 during the whole simulation period 1979–2099, following the ISIMIP2b simulation protocol (2005soc run in Frieler et al., 2017). The impact of CC on irrigation water use was taken into account.

2.4 | Ecologically relevant indicators of wetland water storage regime and its change

We focused on three hydropatterns in each grid cell, (a) mean annual wetland water volume V_m, (b) the (low) wetland water volume V_{90} that is exceeded in 9 out of 10 months and (c) wetland storage range $V_{10} - V_{90}$, with V_{10} being the (high) wetland water volume that is exceeded in only 1 out of 10 months. V_{90} might be critical for the survival of wetland biota, and $V_{10} - V_{90}$ acts as quantification of the ecologically relevant temporal variability of wetland storage. For these three hydropatterns, we computed changes due to WUR during the reference period 1986–2005 by calculating the difference between the volume with WUR (V_{ant}) and the volume without WUR (V_{nat}) in percentage of V_{nat}. CC impacts were similarly quantified, for each GCM–WaterGAP combination, as percent changes between the indicators (with WUR) during the reference period 1986–2015 and 2080–2099. Due to the uncertainties of climate models, bias-correction, and WaterGAP, the evaluation of percent changes is more robust than the evaluation of absolute future values or absolute changes.

2.5 | Reliability of projected CC impacts

To take into account the uncertainty of climate projections, we used the output of three GCMs as input to WaterGAP, and showed the ensemble mean of the relative wetland storage changes computed with the individual GCM outputs. We classified the ensemble mean of projected changes as "reliable" if all three ensemble members had the same sign of change or if the deviating member showed a change between today and the future of less than | 5% | .

We computed the avoidable CC impact as the difference between the impact in case of RCP6.0 (corresponding to a 3 °C GW) and the impact in case of RCP2.6 (2 °C GW), in percent of the impact in case of RCP2.6. Impact was defined as the absolute value of the percent change of a wetland water storage between 1986–2005 and 2080–2099. We classified the ensemble mean of avoidable CC impacts as reliable if the difference between the impacts for both RCPs had the same sign for all three GCMs.

3 | RESULTS

3.1 | Global situation of wetland area and water storage during the reference period 1986–2005

Climatic variations and as well as human water use and reservoirs lead to seasonal and interannual variations of wetland area, such that the mean wetland area during the reference period (A_m) can be much smaller than the maximum area that is likely represented in maps and thus GLWD (Figure 3a,b). The global sum of A_m was 3.178 million km^2, 62% of the global sum of the evaluated maximum wetland area A_{max} of 5.118 million km^2. In most grid cells, A_m is very close to A_{max}. In arid/semiarid regions, however, A_m in percent of A_{max} may even be below 10%, as complete inundation may be restricted to short periods of time (Figure 3b). The sum of A_m in arid/semiarid grid cells of 0.087 million km^2 is only 12% of the sum of A_{max} of 0.723 million km^2. In our study, grid cells are classified as arid/semiarid if the ratio of mean

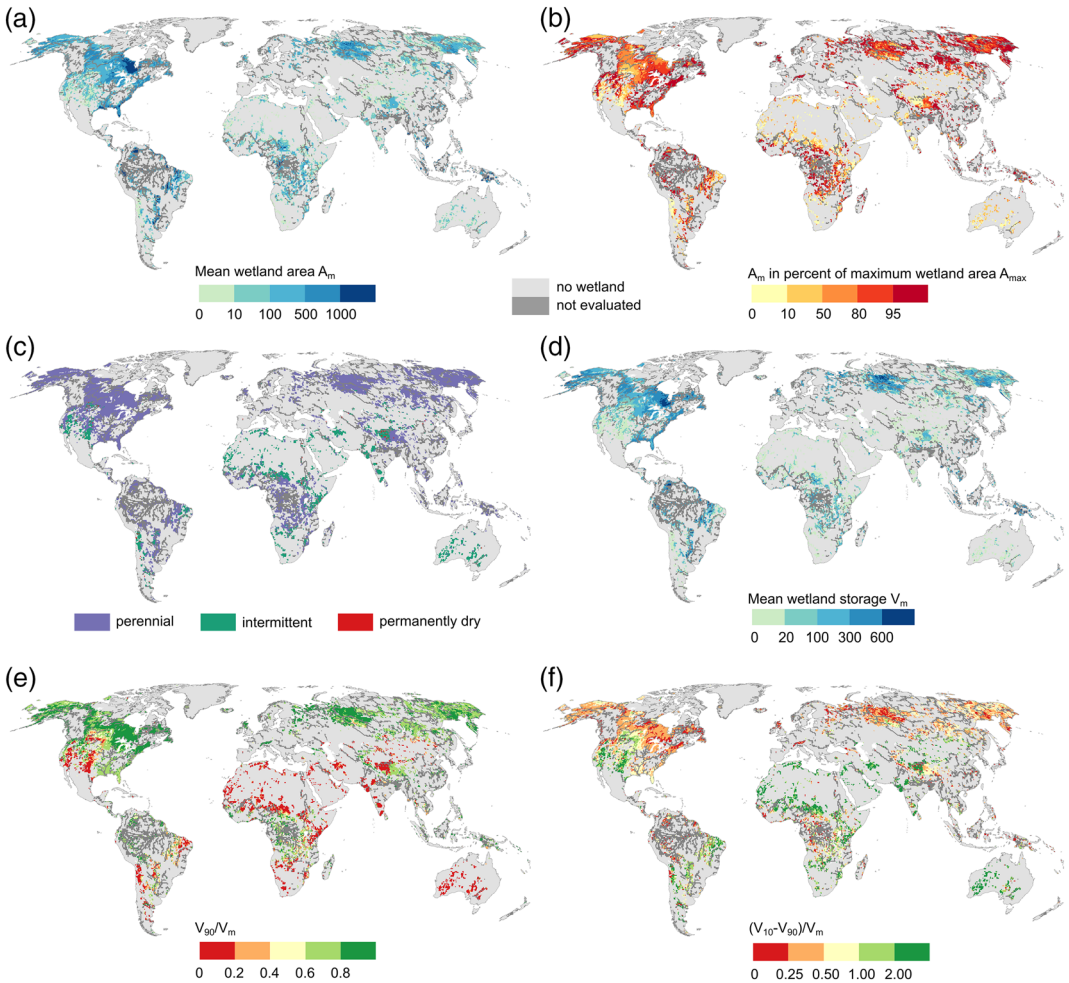

FIGURE 3 Wetland conditions during the reference period 1986–2005 as computed by WaterGAP using observation-based WFDEI climate forcing, taking into account the impact of human water use and reservoirs. Mean wetland area A_m per 0.5° grid cell (with an area of approx. 3,000 km^2 at the equator; square kilometres; a), A_m in percentage of maximum wetland area A_{max} (b), classification of wetlands into perennial, intermittent, and permanently dry wetlands (c), mean wetland water storage V_m (millimetres; d), V_{90}/V_m (e) and $(V_{10} - V_{90})/V_m$. V_{90} the wetland storage that is exceeded in 9 out of 10 months, and V_{10} the storage that is exceeded in 1 out of 10 months

annual precipitation over mean annual potential evapotranspiration is less than 0.5 (except grid cells north of 60° N).

The spatial pattern of A_m in percent of A_{max} (Figure 3b) correlates with the occurrence of perennial, intermittent, and permanently dry wetlands (Figure 3c). Wetland classification was done using monthly time series of the sum of simulated global and local wetland area during the reference period. If wetland area in a grid cell is larger than 1% of A_{GLWD} in all 240 months, the wetlands are classified as permanent. If there is no month with this condition, the wetlands are assumed to be permanently dry. Otherwise, the wetlands are classified as intermittent. Important intermittent wetlands occur in the Western United States, Central South America, and Northeastern Brazil, northern and southern Africa, the Near East, the western and southern parts of India, the western part of Tibet, as well as in Australia (Figure 3c). Permanently dry wetlands are identified in Tibet where the whole region is classified as a wetland complex (Figure 2), whereas in WaterGAP, not enough water is available in those permanently dry cells to keep up a wetland.

As wetland area is simulated in WaterGAP as a function of wetland volume, the spatial pattern of simulated V_m (Figure 3d), expressed in millimetre equivalent water height over the 0.5° grid cell area, is similar to that of A_m (Figure 3a). Temporal variability of wetland water storage is much higher in the dry regions of the globe than in the humid regions. Whereas wetland water storage in dry months V_{90} is within 60–80% of V_m in the humid and subhumid regions of the Earth, V_{90} is less than 20% of V_m in arid/semiarid regions (Figure 3e). Temporal variability of wetland water storage can also be quantified by comparing the range between high and low storage to mean storage. In many of the dry region wetlands, $V_{10} - V_{90}$ is more than twice the value of V_m, whereas in humid area, the range is typically less than 50% of mean storage (Figure 3f). In many regions, however, there is a high spatial heterogeneity of this variability indicator. In the Siberian Ob basin, for example, it varies between less than 25 and 200%, reflecting different snow storage and melt dynamics across the very large region with wetlands. In the central parts of Africa, variability in nearby grid cells even varies between less than 25% to more than 200%.

3.2 | Impact of human water use and man-made reservoirs during the reference period

WUR impact is quantified as the relative difference between wetland water storage in case of WUR and storage V_{m_nat} that would have existed if there had been no WUR during the reference period 1986–2005. Wetlands in arid/semiarid regions, which only cover less than 3% of global A_m, have been more strongly altered by WUR than wetlands in humid regions (Figure 4 and Table 1). On 9.6% of the mean wetland area in arid/semiarid regions, V_{m_nat} was altered by WUR by more than 5%, whereas this was the case on only 3.1% of the global mean wetland area (Table 1, Figure 4a). On 2.5 and 8.2% of global and arid/semiarid A_m, respectively, WUR led to decreases of more than 5%. Decreases are concentrated in arid/semiarid regions with high irrigation water use, in the US, Canada, the Maghreb, Turkey, Iran, Central Asia, India, and Australia. Decreases of more than 25% occurred on 1.7% of the wetland area in arid/semiarid regions, three times the global value. Particularly large decreases of more than 75% are simulated in groundwater depletion area, like the High Plains Aquifer and southern Central Valley in the United States (compare Figure 3 of Döll, Müller Schmied, Schuh, Portmann, & Eicker, 2014 for a map of groundwater depletion) where groundwater outflow to rivers has become zero due to WUR. At the southern tip of India, high surface water abstractions lead to a decrease of wetland water storage (compare Figure 1 of Döll, Fritsche, Eicker, & Müller Schmied, 2014 for maps of net abstractions from groundwater and surface water). A decrease often occurs in response to both groundwater and surface water use. Increases of V_{m_nat} due to WUR of more than 5% affected 0.7% of global A_m. They are very scattered (Figure 4a) and are most likely due to groundwater abstractions with return flows to surface water bodies in upstream cells, for example in the western United States. In terms of relative change, the statistical low volume V_{90} is more strongly affected by WUR than V_m (Table 1, Figure 4b). Decreases of more than 75% due to WUR are widespread and occur also in Southern Africa and South America.

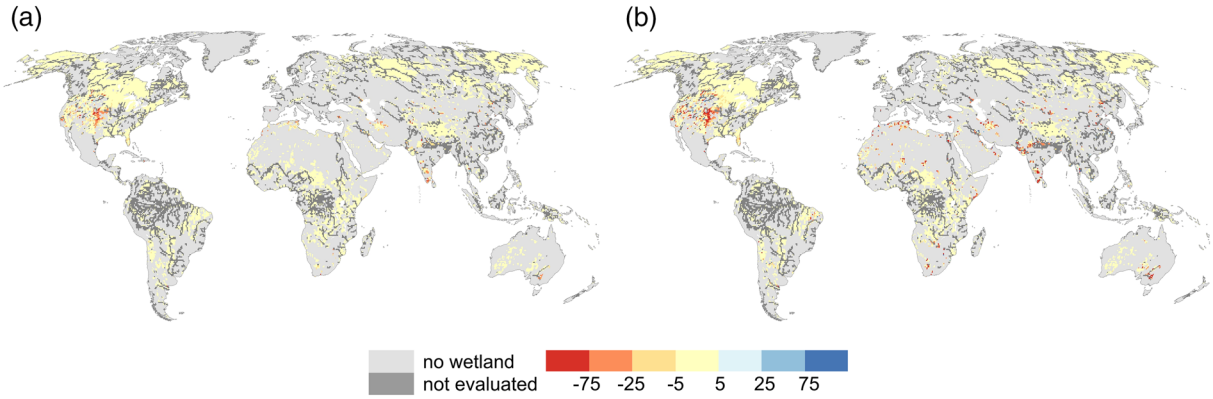

FIGURE 4 Water use and man-made reservoir impact on wetland water storage during 1986–2005. Change in V_m (a) and V_{90} (b) due to human water use and man-made reservoirs in percentage of respective storage under natural conditions $[(V_{ant}-V_{nat})/V_{nat}]$

TABLE 1 Percent of global mean wetland area and mean wetland area in arid/semiarid grid cells A_m, respectively, in reference period 1986–2005 affected by percent changes of three indicators of wetland storage until 2080–2099 under emissions scenarios RCP2.6 and RCP6.0. Only ensemble means of changes are considered. Wetland storage is described by mean storage V_m, low storage V_{90} and an indicator of wetland storage variability, the difference between statistical high and low storage ($V_{10} - V_{90}$). In addition, the percentage of A_m affected by changes due to WUR for the reference period (ref.) is shown (indicators WUR). Global A_m is 3.178 million km^2; A_m in semiarid/arid grid cells is 0.087 million km^2

Indicator	Scenario	less than −25	−25 to −15	−15 to −5	−5 to 5	5–15	15–25	25–100	>100	EM not reliable[a]
Global										
Δ V_m	RCP2.6	1	2.5	8.2	50.5	10.3	1.4	0.6	0	25.4
Δ V_m	RCP6.0	2.3	4.6	11	32.1	18.7	3	1.6	0	26.6
Δ V_{90}	RCP2.6	3.6	3.5	8.6	34.1	9.1	1	0.8	0.1	39.1
Δ V_{90}	RCP6.0	7.8	5.3	11.8	18.9	14.4	2.8	2.2	0.2	36.7
Δ $V_{10} - V_{90}$	RCP2.6	2.8	3.3	8.1	9.6	15.2	8.5	7.9	0.1	44.4
Δ $V_{10} - V_{90}$	RCP6.0	1.9	2.8	4.9	4.8	13.6	13.9	14.1	0.5	43.6
WUR V_m	ref.	0.6	0.3	1.6	96.9	0.5	0.1	0.1	0	n.a.
WUR V_{90}	ref.	1.4	1.0	2.3	93.9	0.6	0.3	0.4	0.1	n.a.
WUR $V_{10} - V_{90}$	ref.	0.5	0.3	0.7	96.4	1.4	0.3	0.3	0	n.a.
Arid/semiarid										
Δ V_m	RCP2.6	5.5	3.7	5.1	3	1.4	4.9	6.7	0.4	69.4
Δ V_m	RCP6.0	6.8	2.8	2.9	2.2	1.5	2.3	4.1	1.1	76.4
Δ V_{90}	RCP2.6	18.5	6.3	2.1	0.7	0.3	0.9	3.8	2.6	64.7
Δ V_{90}	RCP6.0	24.7	2	1	0.4	0	0.7	5	2.1	64
Δ $V_{10} - V_{90}$	RCP2.6	5.6	2.9	3.3	10	3.5	4.1	7.7	1	61.9
Δ $V_{10} - V_{90}$	RCP6.0	5	2.4	2.5	9.7	5.6	1.5	5	2.8	65.5
WUR V_m	ref.	1.7	1.2	5.3	90.4	1.2	0.1	0	0	n.a.
WUR V_{90}	ref.	5.7	2.9	6.3	82.1	1.5	0.2	1.3	0.1	n.a.
WUR $V_{10} - V_{90}$	ref.	1.7	1.2	2.0	89.2	3.5	1.4	0.9	0.1	n.a.

Abbreviations: n.a., not applicable; RCP, Representative Concentration Pathway; WUR, water use and man-made reservoirs.

[a]Ensemble mean not reliable if 1 out of 3 ensemble members has a different sign of change and an absolute change of at least 5%.

3.3 | Projected changes of wetland water storage until the end of the 21st century due to CC

Projected changes of wetland storage due to CC are much larger than the simulated WUR impacts during the reference period 1986–2005, both at the global scale and for arid/semiarid regions (Table 1). Figure 5 includes global maps of percent changes of V_m between the reference period and 2080–2099 for the low-emissions scenario RCP2.6 and the higher-emissions scenario RCP6.0. The results for the individual ensemble members as well as the ensemble mean are provided. Projections by the same climate model for the two RCPs often show an increase in the amount of change from RCP2.6 to RCP6.0, but in some regions there are also opposite signs of change. For example, according to WaterGAP runs with IPSL climate inputs, wetlands in the Sahel and the Middle East become wetter in RCP 2.6 as compared with the reference period and drier in case of RCP6.0. In India, consistent with higher monsoon rainfalls, wetland volumes increase strongly in RCP6.0 whereas in RCP2.6, two wetland regions show drying (Figure 5c,d). With MIROC input, the Pantanal wetland in South America is projected to loose water storage in case of RCP2.6 but gain storage in case of RCP6.0 (Figure 5e,f). Considering the ensemble mean, the majority of the wetland area will only suffer from very small V_m changes of less than 5% in case of RCP2.6 but not RCP6.0 (Figure 5a,b and Table 1). Wetlands in large parts of the northern latitudes are projected to increase in storage with increasing emissions, with the important exception of central Canada. The Mediterranean wetlands that have already been decreased by WUR are projected to decrease even further due to CC. Wetlands in southeastern United States are projected to become slightly wetter in case of RCP2.6 but considerably dryer in case of RCP6.0. It can be reliably estimated that by the end of the century 50% of global wetland area A_m will be spared a significant change in V_m in case of RCP 2.6, whereas this value is reduced to 32% in case of RCP6.0. At the end of the 21st century, there will be slightly more wetland area with increased water storage than with decreased water storage (Table 1).

In case of RCP6.0, 2.3% of global A_m are projected to suffer from a decrease of at least 25% of V_m, a wetland area that is approximately four times larger than the area that suffered such a decrease due to WUR (Table 1). Regarding low wetland storage V_{90}, such a decrease is reliably projected to occur on even 7.8% of global A_m. Temporal variability of wetland water storage is projected to increase with CC. In case of RCP6.0, $V_{10} - V_{90}$ increases by more than 5% on more than

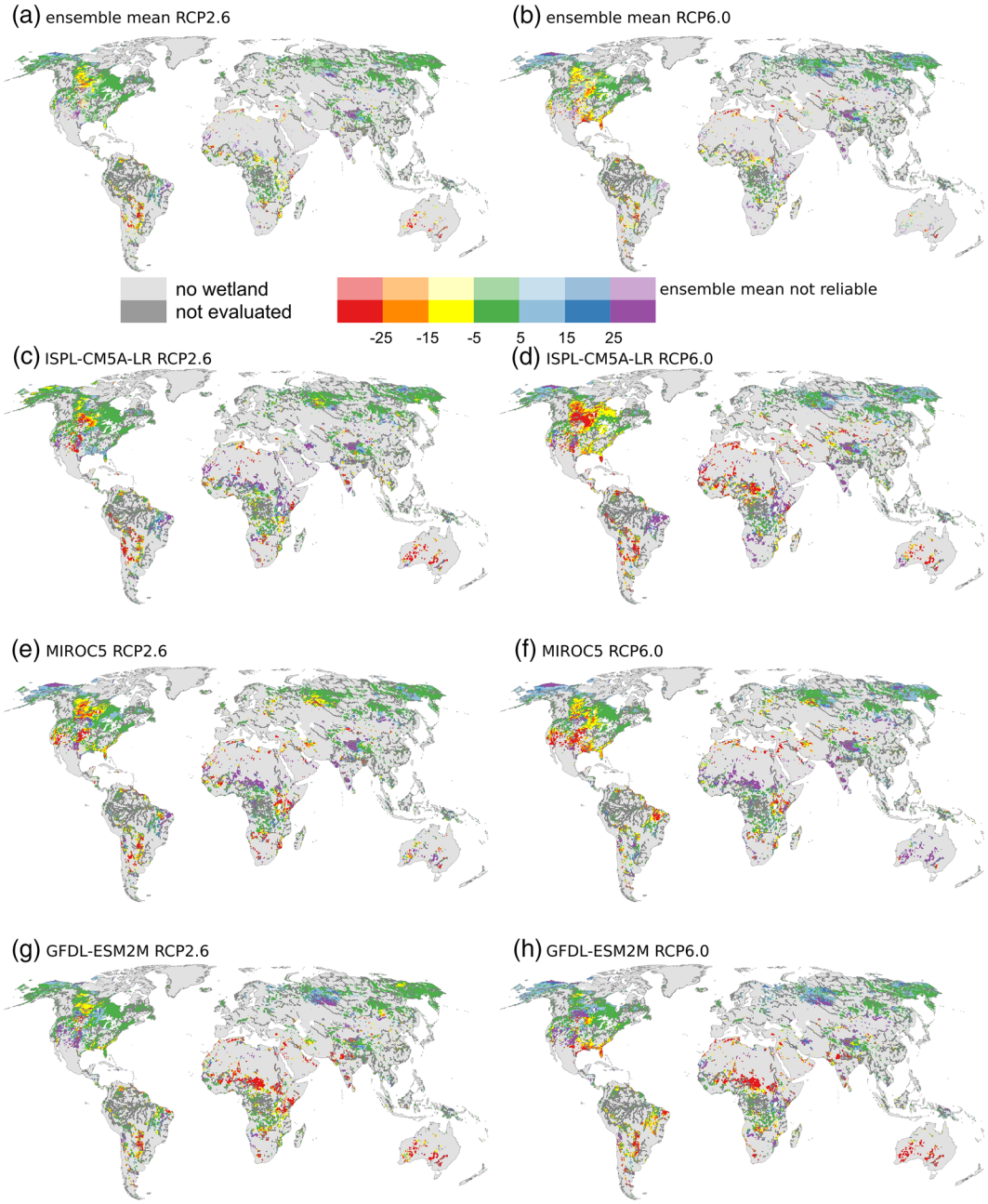

FIGURE 5 Climate change impact on wetland water storage. Percent change of ensemble mean V_m between 1986–2005 and 2080–2099 as computed by WaterGAP driven by the bias-adjusted output of three climate models (ISPL-CM5A-LR, MIROC5, and GFDL-ESM 2M) implementing the greenhouse gas emissions scenarios RCP2.6 (a, c, e, g) and RCP6.0 (b, d, f, h). Projections are defined as "reliable" if changes of all three ensemble members have the same sign or if the deviating ensemble member shows a change of less than $\left|\ 5\%\ \right|$. Reliable ensemble mean changes are shown in bold colours in (a) and (b)

three quarters of the wetlands area with reliable projections, and by more than 25% on 14.6% of the global wetland area (Table 1).

Wetland water storage in arid/semiarid regions will be altered much more strongly by CC than in humid regions. Unfortunately, the results among the three ensemble members vary much more in arid/semi-arid regions than in humid regions so that reliable projections can only be made for a small fraction of A_m (Table 1). Of the 24% of arid/semi-arid wetland area with reliable projections of V_m changes in case of RCP6.0, only 2.2% will have a change of less than $\left|\ 5\%\ \right|$, whereas there will be a significant decrease on 12.5% and a significant increase on 9.0% of the wetland area. V_m decreases of more than 25% are projected to occur at least on 6.8% of the wetland area in arid/semiarid regions by the end of the century. Even worse, a quarter of the semiarid/arid wetland area, and 70% of the area with reliable results, are projected to suffer from a decrease of low water storage V_{90} of more than 25% (Table 1).

To assess how poor countries, which can be assumed to be more vulnerable to environmental changes, are exposed to wetland storage

changes, we evaluated WUR and potential CC impacts on wetland storage indicators separately for four country groups. These groups are composed by countries with similar per-capita gross national income, using the April 2017 World Bank classification of countries into low income, lower middle income, upper middle income, and high income countries (World Bank, 2017). In low-income countries, the wetland area affected by changes in wetland storage of more than 5% due to WUR is, with 7.1%, larger than in the other income groups (2.3–3.6%; Table S1). Interestingly, the wetland area for which reliable projections due to an agreement among climate models can be made is smallest in low-income countries (Table S1). What is striking is that projected decreases in wetland storage strongly dominate increases only in low-income countries, whereas in the other income groups, the sizes of the area with decreasing and increasing wetland storage do not differ much, or the area with increases dominate. In low-income countries, V_m (V_{90}) is projected to decrease under RCP6.0 by more than 5% on 16.4% (29.9%) of the wetland area, and increase on 6.4% (2.4%; Table S1).

An analysis of global totals of wetland water storage is interesting in particular for assessing methane fluxes from wetlands to the atmosphere. During the reference period 1986–2005, WUR did not affect the seasonality (Figure 6a) or interannual variability (Figure 6b) of global V_m but decreased the long-term mean. A comparison of the seasonality of the three GCM-driven runs with the results for the run driven by observation-based WFDEI forcing shows differences even though GCM output was bias-corrected using a climate data set that is very similar to WFDEI. The GCM IPSL-CM5A-LR, for example, results in overall lower values than WFDEI, and a slightly higher seasonality (Figure 6a). All GCMs lead to increased seasonality at the end of this century. Increases of seasonality are higher for RCP6.0 than for RCP2.6. It is striking the interannual variability of global wetland storage is much larger in the GCM-driven runs than in the WFDEI-driven runs (Figure 6b). Consistent with a strong decrease of the low values of mean monthly wetland storage during late summer in case of RCP6.0, IPSL-CM5A-LR shows a clear wetland water storage loss for both the middle and the end of the century. However, an increase of interannual variability of global wetland storage cannot be identified, which may be due to the short 20-year time periods considered. Please remember that 32% of the global maximum wetland area

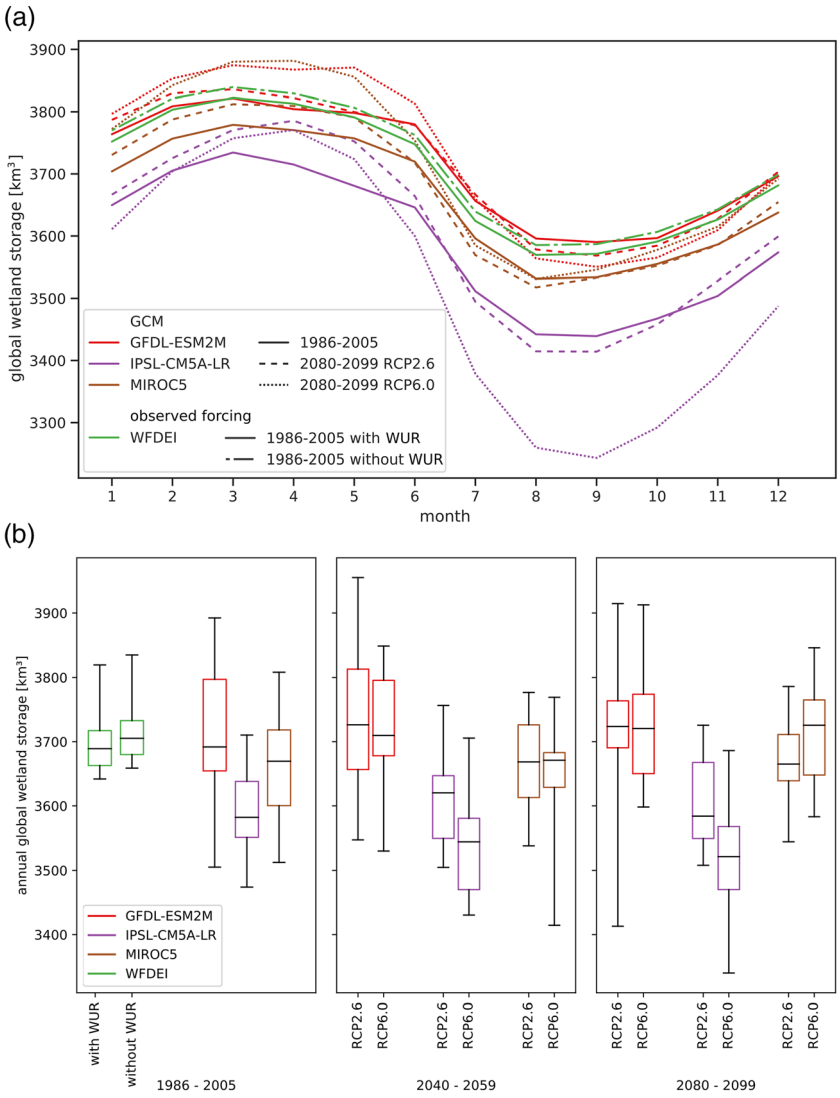

FIGURE 6 Seasonality (a) and interannual variability (b) of global sums of wetland water storage V_m during 1986–2005, 2080–2099 and, in (b), 2040–2059. The four climate forcings of WaterGAP (three GCMs and the observation-based forcing WFDEI) are indicated by colours. Seasonality is shown by mean monthly values over the 20-year periods (a), whereas the box plot shows the distribution of the 20 annual storage values in each time period. The whiskers show the minimum and maximum of the 20 values. GCM, global climate model

TABLE 2 Percent of global wetland area and wetland area in arid/semiarid/grid cells A_m (in reference period 1986–2005) affected by certain levels of avoidable climate change impacts on wetland water storage, as expressed by the difference of impacts for Representative Concentration Pathway (RCP)6.0 and RCP2.6 in percent of the impact for RCP2.6. Only ensemble means of changes are considered

Indicator	Level 0 ≤ 0	Level 1 0–100	Level 2 100–200	Level 3 200–500	Level 4 ≥500	EM not reliable[a]
Global						
V_m	6.1	6.4	7.9	9.4	7	63.3
V_{90}	3.5	5.5	6.5	8.5	7.5	68.5
$V_{10} - V_{90}$	5.7	4.4	5.3	6.6	6.1	72
Arid/semiarid						
V_m	4.8	8.1	5	4.7	4.7	72.6
V_{90}	3.3	6.1	9.2	6	5.7	69.6
$V_{10} - V_{90}$	7.9	5.1	3.7	3.4	4.1	75.7

[a]Ensemble mean not reliable if 1 out of 3 ensemble members has a different sign of change.

considered in WaterGAP, mainly floodplain wetlands, could not be included in this study (see Figure 2).

3.4 | Avoidable CC impacts for wetlands

We define impact as the absolute value of the percent change of a wetland water storage between 1986–2005 and 2080–2099. The avoidable impact is the difference between the impact in case of RCP6.0 (corresponding to a 3 °C GW) and the unavoidable impact in case of RCP2.6 (2 °C), in percent of the impact in case of RCP2.6. We distinguish five levels of avoidable impact (Table 2). In case of Level 0, there is no avoidable impact as the impact under RCP2.6 is smaller than under RCP6.0. In case of Level 1, the impact under RCP6.0 is less than twice the impact under RPC2.6, that is, avoidable impact is less than the unavoidable impact occurring under RCP2.6. For Level 4, the avoidable impact is more than five times larger than the unavoidable one. The ensemble mean of the simulated avoidable impacts regarding V_m can be reliably computed on 36.7% of global A_m (Table 2). On at least 7% of global A_m, the avoidable impact is at Level 4, that is, it is at least five times larger than the impact for RCP2.6., whereas on at least 17.3% is between one to five times larger (Levels 2 and 3). Only on at least 6.4 and 6.1% of the area, the avoided impact is at level 1 and 0, respectively. The values for V_{90} and $V_{10} - V_{90}$ are similar (Table 2), with somewhat smaller land fractions without avoidable impacts in case of V_{90}. Avoidable impacts that are more than five times larger than the unavoidable impacts are found in North America, Siberia, and the Mediterranean (Figure 7). In the former two regions as well as in Central Africa, there are also area where the impact under RCP6.0 is smaller than under RCP2.6, for example, the large wetland in the Ob basin. Avoidable impacts do not differ much among the four country income groups (Table S2).

4 | DISCUSSION

4.1 | Uncertainties

4.1.1 | Identification of wetlands

The difference between a CC impact assessment for wetland storage and for, for example, streamflow is that the former, at least if done at the global scale, is complicated by the lack of a clear definition of "wetland" as well as the partially related lack of a reliable global wetlands data set. In their review of estimates of the global extent of wetlands, Davidson et al. (2018, p. 625) concluded that "we still do not know accurately enough how much wetland remains in the world, or how it is distributed." They urge to improve the extent and quality of information on

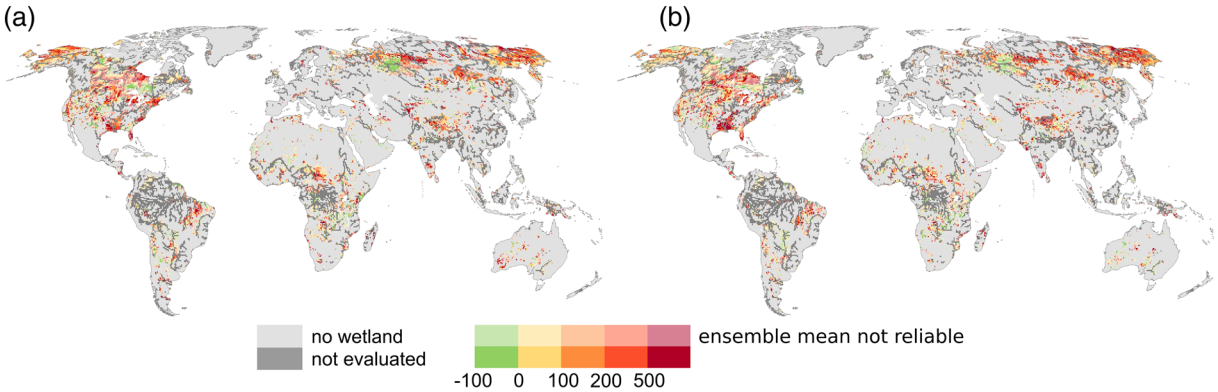

FIGURE 7 Avoidable climate change impacts on wetland water storage, considering mean water storage V_m (a) and of low water storage V_{90}. (b) Ensemble mean of the difference of absolute percent changes between 1986–2005 and 2080–2099 in case of RCP6.0 and RCP2.6, in percentage of the value in case of RCP2.6. If, for example, the avoidable impact is 100%, the absolute percent change of wetland storage in case of RCP6.0 is twice as large as in case of RCP2.6. Negative values indicate that the impact simulated for RCP6.0 is smaller than the impact for RCP2.6. Avoidable impacts are defined as "reliable" if all three ensemble members have the same sign

wetlands through both remote sensing and ground-based comprehensive national wetland inventories that include the type of wetland. Remote sensing approaches are unfortunately limited to detecting open water surfaces (e.g., Pekel et al., 2016) and most remote sensing approaches cannot detect wetlands with inundation under trees or clearly identify noninundated wetlands (Davidson et al., 2018; Schroeder et al., 2015). At the same time, remote sensing approaches cannot distinguish if the open water detected is a lake, a natural wetland, or an inundated rice paddy. Therefore, some studies subsume all these type of open water under the term wetland (e.g., Fluet-Chouinard, Lehner, Rebelo, Papa, & Hamilton, 2015).

Based on multi-sensor remote sensing of the temporal dynamics of inundated area that also identifies inundated area under vegetation (Papa et al., 2010), Fluet-Chouinard et al. (2015) estimated the global wetland area to be at least 12 million km^2 from the mean annual maxima of monthly inundation extent. However, the Papa et al. (2010) data set sometimes overestimates actual inundation as wet soils and vegetation after heavy rainfall may be confounded with inundation, for example, in India and Northwestern Europe (Adam, Döll, Prigent, & Papa, 2010). A comparison of this data set to spatially more highly resolved Landsat 7 Enhanced Thematic Mapper Plus images for the Ganges–Brahmaputra and Paraná river basins as well as for the large Pantanal and Sudd wetlands showed a strong tendency for overestimation of inundated area in particular during and after the rainy season (König, 2011). For a further discussion of the limitations of the Papa et al. (2010) data set, refer to Melton et al. (2013, their section 2.2.3).

Other studies estimated the potential locations and extents of wetlands by computing indices based on precipitation and topography (Hu, Niu, Chen, Li, & Zhang, 2017) or by using the steady-state simulation of distance between land surface and groundwater table of Fan, Li, and Miguez-Macho (2013) to identify groundwater-dependent wetlands (Tootchi et al., 2019). Those studies derived very large global wetland area that are an overestimation of current wetland area due to the extensive man-made wetland losses. For example, both Hu et al. (2017) and Tootchi et al. (2019) identified major parts of the Netherlands and Northwestern Germany as well as the complete Po Valley in northern Italy as wetlands, whereas most of these area cannot be (any longer) considered to be a saturated or inundated wetland. The SWAMP Global Wetlands Map (https://www.cifor.org/global-wetlands/) that claims to show actual wetlands also misclassifies area as wetlands by neglecting the impact of artificial drainage done for gaining agricultural land (e.g., in Albania) or the impact of dams (e.g., the stretch along the Egyptian Nile). In addition, Tootchi et al. (2019) overestimated groundwater-derived wetlands due to a methodological issue. They assumed that the complete area of the 1-km^2 grid cells with a distance to groundwater of less than 0.2 m as computed by Fan et al. (2013) are covered by groundwater-derived wetlands even though most of those grid cells are likely to contain streams that drain the groundwater outflow and lead to an increase of the distance between land surface and groundwater table. In the Fan et al. (2013) global groundwater table simulation, stream–groundwater interaction was not simulated, likely leading to an underestimation of the distance to groundwater.

In summary, it is likely that GLWD applied in this study misses a significant number of wetlands around the globe that existed during the reference period but were not mapped but many more recent estimations likely overestimate wetland area. It does not appear to be reasonable to base the simulation of current and future wetland dynamics on data sets of potential wetlands such as Hu al. (2017) and Tootchi et al. (2019) unless wetland loss from natural conditions due to artificial drainage and other human impacts is simulated, too.

4.1.2 | Simulation of wetland dynamics

Land surface models as components of global climate models simulate wetlands quite differently from WGHM. Among the nine global models participating in the Wetland CH4 Inter-comparison of Models Project (WETCHIMP), four relied on prescribed wetland area whereas the others simulated the dynamics of wetland area in order to simulate methane fluxes (Wania et al., 2013). The global sums of wetland area varied strongly among the models, from 2.7–34.9 million km^2. Whereas WGHM simulates all wetlands similar to lakes as a body of water, some WETCHIMP models distinguish between inundated wetlands and noninundated wetlands (in particular peat), with noninundated wetlands being simulated as highly saturated soil (Wania et al., 2013). In case of the land surface models JULES and ORCHIDEE, the wetland fraction of each grid cell is estimated as a function of the simulated groundwater table and a topographic index (TOPMODEL approach; Comyn-Platt et al., 2018; Wania et al., 2013). In WaterGAP, however, a groundwater table is not simulated as it is difficult to plausibly simulate the groundwater table without considering lateral groundwater flows (not simulated by JULES or ORCHIDEE either). As WaterGAP does not aim at modelling methane fluxes from wetlands but the impact of wetlands on water flows, the focus is on estimating water storage dynamics, with areal dynamics being computed as a simple function of wetland storage (Equation 3).

In the presented study, unfortunately we had to disregard 31.7% of the GLWD wetland area considered in WaterGAP as the model is currently not able to simulate storage dynamics appropriately in these grid cells with global wetlands. These wetlands are either "floodplain"/"flooded forest" wetlands like the Amazon wetlands that are fed from overflowing river channels or narrow floodplains along large rivers (river wetlands, Lehner & Döll, 2004). Simulation of these floodplain wetlands with a globally constant maximum water table elevation range of 2-m leads for many of these wetlands to a constant water storage at its maximum. A more plausible simulation of wetland storage dynamics of floodplain/flooded forest wetlands could be achieved by spatially varying the maximum range, for example, to 20 m for the Amazon basin (Adam, 2017), possibly by model calibration. River wetlands of GLWD should not be simulated with the current wetland storage algorithm. Alternatively, the current algorithm for global wetlands in WaterGAP could be replaced by simulating inundation of floodplains taking into account topography and estimates of bankfull flow (Adam, 2017; Decharme et al., 2012; Ringeval et al., 2014; Yamazaki, Kanae, Kim, & Oki, 2011). The latter approach is preferable but computationally expensive, and it suffers from the rather poor

accuracy of global digital elevation models, in particular in cases of forest cover.

Simulation of water storage and area dynamics of the more than 5 million km^2 of wetlands evaluated in the study is hampered by a number of methodological constraints. Increase of wetland area beyond A_{GLWD} and increase of wetland water storage beyond S_{wmax} (2 m × A_{max}) cannot be simulated. Wetlands such as bogs that depend on precipitation as the dominant water source may not be simulated well as in WaterGAP wetlands are fed by surface water, too, and in humid area also by groundwater. In WaterGAP, the effect of permafrost melting on wetlands is not taken into account (and is uncertain according to Junk et al., 2013). The impact of man-made reservoirs on wetland is likely underestimated as only the impact of the 1,109 largest reservoirs (including regulated lakes) is taken into account. As wetland area is derived from storage using a simple, globally homogeneous function, the uncertainty of area dynamics is expected to be larger than the uncertainty of storage dynamics.

Finally, loss of wetland storage until the reference period is not taken into account. This is due to the fact that GLWD wetland data are used for identifying location and maximum extent of wetlands, and GLWD only includes wetlands that still existed in second half of the 20th century. The dominant reason for wetland losses was artificial drainage to gain agricultural and grazing land (Van Asselen, Verburg, Vermaat, & Janse, 2013). Therefore, a global map of artificially drained area (Figure A1a, Feick, Siebert, & Döll, 2005) helps to estimate where wetlands may have existed but had already been desiccated due to artificial drainage before the maps that form the basis of GLWD were created. For example, large area in Great Britain, Northern Germany, and Poland were originally covered by fens that were later drained and therefore do not appear as wetlands in GWLD. About half of the global artificially drained area of 1.67 million km^2 are rainfed cropland, the other half irrigated, with large variations among countries (Fig A1b, Feick et al., 2005). It can be assumed that large parts of the drained rainfed cropland were formerly wetlands, in particular fens and peatland.

4.1.3 | Assessment of CC impacts on wetland water storage

CC impact assessments suffer from both the uncertainty of the global climate models and the uncertainty of the impact model (here: global hydrological model; Hagemann et al., 2013). To take into account, at least to a certain extent, the uncertainty of global climate models, we applied bias-adjusted output of three global climate models. To analyse an ensemble of multiple global hydrological models is currently very difficult due to the differing wetland distributions among the various global hydrological models or the lack of wetland modelling in some.

Not surprisingly, the three WaterGAP model runs driven by the climate scenarios of three global climate models vary strongly regarding the evaluated relative changes in wetland water storage (Figure 5). The mean of the three relative changes can be considered more robust than the individual members and is therefore presented in Figures 5 and 7 as well as Tables 1 and 2. There, discrepancies in the sign of change among the three were taken into account when presenting the mean, leading to a very rough classification into reliable and nonreliable grid cell-specific indicator changes. In case of the storage change indicators, the fraction of the global wetland area with reliable changes differed according to the indicators considered. Interestingly, it is much smaller in semiarid/arid climate than in other climate zones, and does not change with increased GW (Table 1).

4.2 | Implications for CC mitigation and adaptation

The study quantifies the avoidable CC impacts on wetland water storage as the difference between the absolute values of percent changes of storage indicators for RCP6.0 and RCP2.6 in percentage of the value for RCP2.6. Here, it was assumed that the stronger the deviation from current conditions is, independent of the sign, the stronger is the CC impact. Mainly due to climate model uncertainty, avoidable impacts can only be quantified reliably for 28–37% of the evaluated global wetland area (Table 2). On 18–24% of the wetland area, the avoidable impact at the end of the 21st century is reliably computed to be larger than the impact for RCP2.6, and on 6–7% even five times as large (Table 2). Only for 4–6% of the wetland area, there is no avoidable impact as the simulated impact under RCP2.6 is larger than under RCP 6.0. Thus, despite climate model uncertainties, this study establishes that avoidable CC impacts for wetland water storage are important in magnitude, thus supporting a strong CC mitigation.

Regarding adaptation to CC, the study indicates likely future trends of wetland storage in different area of the globe that can be used to optimize efforts of wetland conservation and restoration (Kingsford, 2011). For example, efforts for wetland restoration should focus on regions in which stable or increasing wetland water storage is likely for the future (Johnson et al., 2005). If wetlands that have already decreased in size by human water use are projected to suffer from an additional decrease of wetland storage due to CC, a reduction in human water use is appropriate for adapting to CC. Information on changes in wetland storage and area can be used locally to derive changes in habitat quality for water fowl (Johnson et al., 2005) or fish, which may allow a more targeted adaptation management. Special attention should be given to adaptation efforts regarding wetland loss in semiarid/arid regions and low income countries as they will be more exposed to losses than to gains of wetland water storage and area than humid regions and wealthier countries, respectively.

5 | CONCLUSIONS

According to simulations with the global hydrological model WaterGAP, temporal variability of wetland water storage and extent increases strongly with aridity, as is expected. Intermittent wetlands that fell dry for at least 1 month during the reference period 1986–2005 were identified in many arid and semiarid regions of the globe. Of the analysed wetland area in arid/semiarid regions, 8% suffered from a relevant decrease in mean water storage of more than 5%

during the reference period due to human water and man-made reservoirs, mainly irrigation, as compared with natural conditions, with decreases of more than 75% in some groundwater depletion area. Wetlands in humid area were hardly affected by these human activities but by artificial drainage to gain agricultural land. However, this could not be analysed in this study due to lack of data.

Severe wetland water storage losses due to human water use and reservoirs in the Mediterranean, the Near East, and Australia are projected to be exacerbated by CC, whereas climate models do not agree regarding the future of equally impacted wetlands in the USA. Future CC will lead to much larger and widespread changes of wetland water storage dynamics than human water use and reservoirs did in the past, even in arid/semiarid regions and 2 °C GW. In case of 2 °C GW, only half of the global wetland area analysed in this study is reliably estimated to be unaffected by significant water storage changes of more than 5%, whereas this is true for only one third in case of a 3 °C warming. Globally, a slightly higher wetland area is projected to increase in mean water storage than decrease due to CC, whereas the reverse is true for the low water storage that is exceeded in 9 out of 10 months. Most wetlands will experience a higher temporal variability of water storage due to CC.

Wetlands in arid/semiarid regions are projected to suffer much higher relative changes of wetland water storage and area than wetlands in humid area. Only a very small fraction will remain unaffected by significant changes. A quarter of the arid/semi-arid wetland area, and 70% of the area with reliable results, are projected to suffer from a decrease of low water storage V_{90} of even more than 25%. Different from the more wealthy country income groups, wetlands in low-income countries are projected to dominantly loose water storage due to CC, while projections for these countries suffer from the highest uncertainty.

The wetland area that will be affected by significant changes in wetland storage clearly increases from 2 °C to 3 °C GW. Avoidable CC impacts, that is, the additional impacts of a 3 °C GW as compared with those already occurring for a 2 °C GW, are large, mostly more than two times larger than the impacts in case of 2 °C GW. However, due to climate model uncertainty, avoidable impacts can only be computed reliably for about 30% of the wetland area. Please note that emissions reduction pledges that governments made in the framework of the international climate negotiations as of December 2018 would limit GW to only about 3 °C (Climate Action Tracker, 2019).

To improve national to global-scale assessments of CC impacts on wetlands, development of a comprehensive global wetlands data set including location, type, and extent is paramount. Assessment of floodplain wetlands that had to be excluded from this study will be possible if the dynamics of floodplain inundation by overbank flows can be reliably simulated.

ACKNOWLEDGEMENTS

We thank Hans-Peter Rulhof-Döll for preparing Figure A1. We are very grateful for the comments of two anonymous reviewers that helped us to improve the manuscript.

AUTHOR CONTRIBUTIONS

PD conceived the study, designed the methodology and wrote the original draft of the manuscript. MG and TT performed the investigation. TT also did formal analysis and visualization, while HMS contributed to methodology and software. All co-authors contributed to the formulation of the final manuscript.

DATA ACCESSIBILITY

The data that support the findings of this study are available from the corresponding author upon reasonable request.

ORCID

Petra Döll https://orcid.org/0000-0003-2238-4546
Tim Trautmann https://orcid.org/0000-0001-8652-6836
Hannes Müller Schmied https://orcid.org/0000-0001-5330-9923

REFERENCES

Adam, L. (2017). Modeling water storage dynamics in large floodplains and wetlands. In Frankfurt Hydrology Paper, *17*, *Institute of Physical Geography*, *Goethe University Frankfurt*. Frankfurt am: Main, Germany.

Adam, L., Döll, P., Prigent, C., & Papa, F. (2010). Global-scale analysis of satellite-derived time series of naturally inundated area as a basis for floodplain modelling. *Advances in Geosciences*, *27*, 45–50. https://doi.org/10.5194/adgeo-27-45-2010

Brander, L. M., Bräuer, I., Gerdes, H., Ghermandi, A., Kuik, O., Markandya, A., … Wagtendonk, A. (2012). Using meta-analysis and GIS for value transfer and scaling up: valuing climate change induced losses of European wetlands. *Environmental and Resource Economics*, *52*, 395–413. https://doi.org/10.1007/s10640-011-9535-1

Comyn-Platt, E., Hayman, G., Huntingford, C., Chadburn, S. E., Burke, E. J., Harper, A. B., … Sitch, S. (2018). Carbon budgets for 1.5 and 2 °C targets lowered by natural wetland and permafrost feedbacks. *Nature Geoscience*, *11*, 568–573. https://doi.org/10.1038/s41561-018-0174-9

Davidson, N. C. (2014). How much wetland has the world lost? Long-term and recent trends in global wetland area. *Marine and Freshwater Research*, *65*, 934–941. https://doi.org/10.1071/MF14173

Davidson, N. C., Fluet-Chouinard, E., & Finlayson, C. M. (2018). Global extent and distribution of wetlands: trends and issues. *Marine and Freshwater Research*, *69*, 620–627. https://doi.org/10.1071/MF17019_AC

Decharme, B., Alkama, R., Papa, F., Faroux, S., Douville, H., & Prigent, C. (2012). Global off-line evaluation of the ISBA-TRIP flood model. *Climate Dynamics*, *38*(7–8), 1389–1412. https://doi.org/10.1007/s00382-011-1054-9

Döll, P., & Bunn, S. E. (2014). Cross-chapter box on the impact of climate change on freshwater ecosystems due to altered river flow regimes. In: Climate change 2014: Impacts, adaptation, and vulnerability. *Part A: Global and sectoral aspects. Contribution of Working Group II to the Fifth Assessment Report of the Intergovernmental Panel on Climate Change* [Field, C. B., Barros, V. R., Dokken, D. J., Mach, K. J., Mastrandrea, M. D., Bilir, T. E., Chatterjee, M., Ebi, K. L., Estrada, Y. O., Genova, R. C., Girma, B., Kissel, E. S., Levy, A. N., MacCracken, S., Mastrandrea, P. R., & White, L.L. (eds.)]. Cambridge University Press, Cambridge, United Kingdom and New York, NY, USA, 143–146.

Döll, P., Douville, H., Güntner, A., Müller Schmied, H., & Wada, Y. (2016). Modelling freshwater resources at the global scale: Challenges and

prospects. *Surveys in Geophysics*, *37*(2), 195–221. https://doi.org/10.1007/s10712-015-9343-1

Döll, P., Fiedler, K., & Zhang, J. (2009). Global-scale analysis of river flow alterations due to water withdrawals and reservoirs. *Hydrology and Earth System Sciences*, *13*, 2413–2432. https://doi.org/10.5194/hess-13-2413-2009

Döll, P., Fritsche, M., Eicker, A., & Müller Schmied, H. (2014). Seasonal water storage variations as impacted by water abstractions: Comparing the output of a global hydrological model with GRACE and GPS observations. *Surveys in Geophysics*, *35*(6), 1311–1331. https://doi.org/10.1007/s10712-014-9282-2

Döll, P., Jiménez-Cisneros, B., Oki, T., Arnell, N., Benito, C., Cogley, G., … Nishijima, A. (2015). Integrating risks of climate change into water management. *Hydrological Sciences Journal*, *60*(1), 3–14. https://doi.org/10.1080/02626667.2014.967250

Döll, P., Müller Schmied, H., Schuh, C., Portmann, F., & Eicker, A. (2014). Global-scale assessment of groundwater depletion and related groundwater abstractions: Combining hydrological modeling with information from well observations and GRACE satellites. *Water Resources Research*, *50*, 5698–5720. https://doi.org/10.1002/2014WR015595

Fan, Y., Li, H., & Miguez-Macho, G. (2013). Global patterns of groundwater table depth. *Science*, *339*, 940–943. https://doi.org/10.1126/science.1229881

Fan, Y., & Miguez-Macho, G. (2011). A simple hydrologic framework for simulating weltands in climate and earth system models. *Climate Dynamics*, *37*, 253–278. https://doi.org/10.1007/s00382-010-0829-8

Feick, S., Siebert, S., & Döll, P. (2005). A digital global map of artificially drained agricultural area. In *Frankfurt Hydrology Paper 04*, *Institute of Physical Geography*, *Goethe University Frankfurt* (p. 57). Frankfurt am: Main, Germany. http://www.uni-frankfurt.de/53949648/Frankfurt_Hydrology_Papers

Finlayson, C. M., D´Cruz, R., Aladin, N., Barker, D. R., Beltram, G., Brouwer, J., … Toryannikova, R. (2005). Inland Water Systems. In R. Hassan, R. Scholer, & N. Ash (Eds.), *Ecosystems and human well-being: Current state and trends* (Vol. 1) (pp. 551–583). Washington: Island Press.

Fluet-Chouinard, E., Lehner, B., Rebelo, L.-M., Papa, F., & Hamilton, S. K. (2015). Development of a global inundation map at high spatial resolution from topographic downscaling of coarse-scale remote sensing data. *Remote Sensing of Environment*, *158*, 348–361. https://doi.org/10.1016/J.RSE.2014.10.015

Frieler, K., Lange, S., Piontek, F., Reyer, C. P. O., Schewe, J., Warszawski, L., … Yamagata, Y. (2017). Assessing the impacts of 1.5 °C global warming—Simulation protocol of the Inter-Sectoral Impact Model Intercomparison Project (ISIMIP2b). *Geoscientific Model Development*, *10*, 4321–4345. https://doi.org/10.5194/gmd-10-4321-2017

Gudmundsson, L., Tallaksen, L. M., Stahl, K., Clark, D. B., Dumont, E., Hagemann, S., … Koirala, S. (2012). Comparing large-scale hydrological model simulations to observed runoff percentiles in Europe. *Journal of Hydrometeorology*, *13*, 604–620. https://doi.org/10.1175/JHM-D-11-083.1

Hagemann, S., Chen, C., Clark, D. B., Folwell, S., Gosling, S. N., Haddeland, I., … Wiltshire, A. J. (2013). Climate change impact on available water resources obtained using multiple global climate and hydrology models. *Earth System Dynamics*, *4*, 129–144. https://doi.org/10.5194/esd-4-129-2013

Hu, S., Niu, Z., Chen, Y., Li, L., & Zhang, H. (2017). Global wetlands: Potential distribution, wetland loss, and status. *Science of the Total Environment*, *586*, 319–327. https://doi.org/10.1016/j.scitotenv.2017.02.001

Hunger, M., & Döll, P. (2008). Value of river discharge data for global-scale hydrological modelling. *Hydrology and Earth System Sciences*, *12*, 841–861. https://doi.org/10.5194/hess-12-841-2008

IPCC (2013). In T. F. Stocker, D. Qin, G.-K. Plattner, M. Tignor, S. K. Allen, J. Boschung, et al. (Eds.), *Summary for Policymakers. In: Climate change 2013: The physical science basis. contribution of working group I to the Fifth Assessment Report of the Intergovernmental Panel on Climate Change* (pp. 1–29). Cambridge, United Kingdom and New York, NY, USA: Cambridge University Press.

IPCC (2014). In C. B. Field, V. R. Barros, D. J. Dokken, K. J. Mach, M. D. Mastrandrea, T. E. Bilir, et al. (Eds.), *Summary for policymakers. In: Climate change 2014: Impacts, adaptation, and vulnerability. Part A: Global and sectoral aspects. Contribution of Working Group II to the Fifth Assessment Report of the Intergovernmental Panel on Climate Change* (pp. 1–32). Cambridge, United Kingdom and New York, NY, USA: Cambridge University Press.

Jackson, C. R., Thompson, J. A., & Kolka, R. K. (2014). Wetland soils, hydrology, and geomorphology. In D. P. Batzer, & R. R. Sharitz (Eds.), *Ecology of freshwater and estuarine wetlands* (Second ed.) (pp. 23–60). Oakland, CA, USA: University of California Press.

Johnson, W. C., Millett, B. V., Gilmanov, T., Voldseth, R. A., Guntenspergen, G. R., & Naugle, D. E. (2005). Vulnerability of northern prairie wetlands to climate change. *Bioscience*, *55*(10), 863–872.

Junk, W. J., An, S., Finlayson, C. M., Gopal, B., Kvêt, J., Mitchell, S. A., … Robarts, R. D. (2013). Current state of knowledge regarding the world's wetlands and their future under global climate change: A synthesis. *Aquatic Sciences*, *75*, 151–167. https://doi.org/10.1007/s00027-012-0278-z

Keddy, P. A. (2000). *Wetland ecology: Principles and conservation*. Cambridge, U.K.: Cambridge University Press.

Kingsford, R. T. (2011). Conservation management of rivers and wetlands under climate change—A synthesis. *Marine and Freshwater Research*, *62*(3), 217–222.

König, M. (2011). *Validierung einer globalen Zeitreihe der terrestrischen Wasserbedeckung (Validation of a global time series of terrestrial inundation extent)*. Germany: Unpublished diploma thesis, Institute of Physical Geography, Goethe University Frankfurt.

Laboratory, E. (1987). Corps of Engineers wetlands delineation manual. In *Technical report Y-87-1*. Vicksburg, MS: U.S. Army Engineer Waterways Experiment Station.

Lange, S. (2017). ISIMIP2b bias-correction fact sheet. Potsdam Institute for Climate Research. (https://www.isimip.org/gettingstarted/isimip2b-bias-correction/)

Lehner, B., & Döll, P. (2004). Development and validation of a database of lakes, reservoirs and wetlands. *Journal of Hydrology*, *296*(1-4), 1–22. https://doi.org/10.1016/j.jhydrol.2004.03.028

Lehner, B., Reidy Liermann, C., Revenga, C., Vörösmary, C., Fekete, B., Crouzet, P., … Wisser, D. (2011). High resolution mapping of the world's reservoirs and dams for sustainable river flow management. *Frontiers in Ecology and the Environment*, *9*(9), 494–502.

Melton, J.R., Wania, R., Hodson, E.L., Poulter, B., Ringeval, B., Spahn, R., … Kaplan, J.O. (2013). Present state of global wetland extent and wetland methane modelling: conclusions from a model intercomparison project (WETCHIMP). *Biogeosciences*, *10*, 753–788. https://doi.org/10.5194/bg-10-753-2013

Mendelssohn, I. A., Batzer, D. P., Holt, C., & Graham, S. A. (2014). Abiotic constraints for wetland plants and animals. In D. P. Batzer, & R. R. Sharitz (Eds.), *Ecology of freshwater and estuarine wetlands* (Second ed.) (pp. 61–86). Oakland, CA, USA: University of California Press.

Mitsch, W. J., Bernal, B., Nahlik, A. M., Mander, U., Zhang, L., Anderson, C. J., … Brix, H. (2013). Wetlands, carbon, and climate change. *Landscape Ecology*, *28*, 583–597.

Müller Schmied, H., Adam, L., Eisner, S., Fink, G., Flörke, M., Kim, H., … Döll, P. (2016). Variations of global and continental water balance components as impacted by climate forcing uncertainty and human water use. *Hydrology and Earth System Sciences*, *20*, 2877–2898. https://doi.org/10.5194/hess-20-2877-2016

Müller Schmied, H., Eisner, S., Franz, D., Wattenbach, M., Portmann, F. T., Flörke, M., & Döll, P. (2014). Sensitivity of simulated global-scale freshwater fluxes and storages to input data, hydrological model structure, human water use and calibration. *Hydrology and Earth System Sciences*, *18*, 3511–3538. https://doi.org/10.5194/hess-18-3511-2014

Papa, F., Prigent, C., Jimenez, C., Aires, F., Rossow, W. B., & Matthews, E. (2010). Interannual variability of surface water extent at global scale, 1993-2004. *Journal of Geophysical Research*, *115*(D12111), 2010. https://doi.org/10.1029/2009JD012674

Pekel, J.-F., Cottam, A., Gorelick, N., & Belward, A. S. (2016). High resolution mapping of global surface water and its long-term changes. *Nature*, 1–19. https://doi.org/10.1038/nature20584

Ringeval, B., Houweling, S., van Bodegom, P. M., Spahni, R., van Beek, R., Joos, F., & Rückmann, T. (2014). Methane emissions form floodplains in the Amazon basin: Challenges in developing a process-based model for global applications. *Biogeosciences*, *11*, 1519–1558. https://doi.org/10.5194/bg-11-1519-2014

Schneider, C., Flörke, M., de Stefano, L., & Petersen-Perlman, J. D. (2017). Hydrological threats to riparian wetlands of international importance—A global quantitative and qualitative analysis. *Hydrology and Earth System Sciences*, *21*(6), 2799–2815.

Schroeder, R., McDonald, K. C., Chapman, B. C., Jensen, K., Podest, E., Tessler, Z. D., … Zimmermann, R. (2015). Developmet and evaluation of a multi-year fractional surface water data set derived from active/passive microwave remote sensing data. *Remote Sensing*, *7*, 16688–16732. https://doi.org/10.3390/rs71215843

Settele, J., Scholes, R., Betts, R., Bunn, S., Leadley, P., Nepstad, D., … Taboada, M. A. (2014). In C. B. Field, V. R. Barros, D. J. Dokken, K. J. Mach, M. D. Mastrandrea, T. E. Bilir, et al. (Eds.), *Terrestrial and inland water systems. In: Climate change 2014: Impacts, adaptation, and vulnerability. Part A: Global and sectoral aspects. Contribution of Working Group II to the Fifth Assessment Report of the Intergovernmental Panel on Climate Change* (pp. 271–359). Cambridge, United Kingdom and New York, NY, USA: Cambridge University Press.

Sharitz, R. R., Batzer, D. P., & Pennings, S. C. (2014). Ecology of freshwater and estuarine wetlands: An introduction. In D. P. Batzer, & R. R. Sharitz (Eds.), *Ecology of freshwater and estuarine wetlands. Second edition* (pp. 1–22). Oakland, CA, USA: University of California Press.

Stacke, T., & Hagemann, S. (2012). Development and evaluation of a global dynamical wetlands extent scheme. *Hydrology and Earth System Sciences*, *16*, 2915–2933. https://doi.org/10.5194/hess-16-2915-2012

Tallaksen, L. M., & Stahl, K. (2014). Spatial and temporal patterns of large-scale droughts in Europe: model dispersion and performance. *Geophysical Research Letters*, *41*, 429–434.

Tootchi, A., Jost, A., & Ducharne, A. (2019). Multi-source global wetland maps combining surface water imagery and groundwater constraints. *Earth System Science Data*, *11*, 189–220.

Climate Action Tracker (2019). https://climateactiontracker.org/global/temperatures/

Twilley, R. R., & Brinson, M. M. (2014). Consequences for wetlands of a changing global environment. In D. P. Batzer, & R. R. Sharitz (Eds.), *Ecology of freshwater and estuarine wetlands* (Second ed.) (pp. 261–286). Oakland, CA, USA: University of California Press.

Van Asselen, S., Verburg, P. H., Vermaat, J. E., & Janse, J. H. (2013). Drivers of wetland conversion: A global meta-analysis. *PLoS ONE*, *8*, e81292. https://doi.org/10.1371/journal.pone.0081292

Veldkamp, T. I. E., Zhao, F., Ward, P. J., de Moel, H., Aerts, J. C. J. H., Müller Schmied, H., … Wada, Y. (2018). Human impact parameterizations in global hydrological models improve estimates of monthly discharges and hydrological extremes: A multi-model validation study. *Environmental Research Letters*, *13*, 055008. https://doi.org/10.1088/1748-9326/aab96f

Wania, R., Melton, J., Hodson, E., Poulter, B., Ringeval, B., Spahni, R., … Kaplan, P. (2013). Present state of global wetland extent and wetland methane modelling: Methodology of a model intercomparison project (WETCHIMP). *Geoscientific Model Development*, *6*, 617–641. https://doi.org/10.5194/gmd-6-617-2013

Weedon, G. P., Balsamo, G., Bellouin, N., Gomes, S., Best, M. J., & Viterbo, P. (2014). The WFDEI meteorological forcing data set: WATCH Forcing Data methodology applied to ERA-Interim reanalysis data. *Water Resources Research*, *50*, 7505–7514. https://doi.org/10.1002/2014WR015638

World Bank (2017). World Bank country and lending groups (https://datahelpdesk.worldbank.org/knowledgebase/articles/906519)

Yamazaki, D., Kanae, S., Kim, H., & Oki, T. (2011). A physically based description of floodplain inundation dynamics in a global river routing model. *Water Resources Research*, *47*, W04501. https://doi.org/10.1029/2010WR009726

Zaherpour, J., Gosling, S. N., Mount, N., Müller Schmied, H., Veldkamp, T. I. E., Dankers, R., … Wada, Y. (2018). Worldwide evaluation of mean and extreme runoff from six global-scale hydrological models that account for human impacts. *Environmental Research Letters*, *13*, 065015. https://doi.org/10.1088/1748-9326/aac547

SUPPORTING INFORMATION

Additional supporting information may be found online in the Supporting Information section at the end of the article.

How to cite this article: Döll P, Trautmann T, Göllner M, Müller Schmied H,. A global-scale analysis of water storage dynamics of inland wetlands: Quantifying the impacts of human water use and man-made reservoirs as well as the unavoidable and avoidable impacts of climate change. *Ecohydrology*. 2020;13:e2175. https://doi.org/10.1002/eco.2175

APPENDIX A

GLOBAL DATA SET OF ARTIFICIAL DRAINAGE

Artificial drainage serves to lower the groundwater table of wetland like fens (e.g., in Northern Germany and Poland), thus degrading and destroying them. Therefore, artificial drainage indicates the previous existence of wetlands unless the purpose of artificial drainage is to keep the groundwater table from rising due to infiltration of irrigation water, to avoid soil salination. These two purposes of artificial drainage could not be distinguished in the global data set of artificial drainage of Feick et al. (2005) shown in Figure A1a. For many countries, data on drained rainfed agricultural area, which would more clearly indicate wetland loss, are not available (Figure A1b). The larger the fraction of drained rainfed agriculture (Figure A1b), the more likely it is that part of the area with artificial drainage shown in Figure A1a was formerly a wetland.

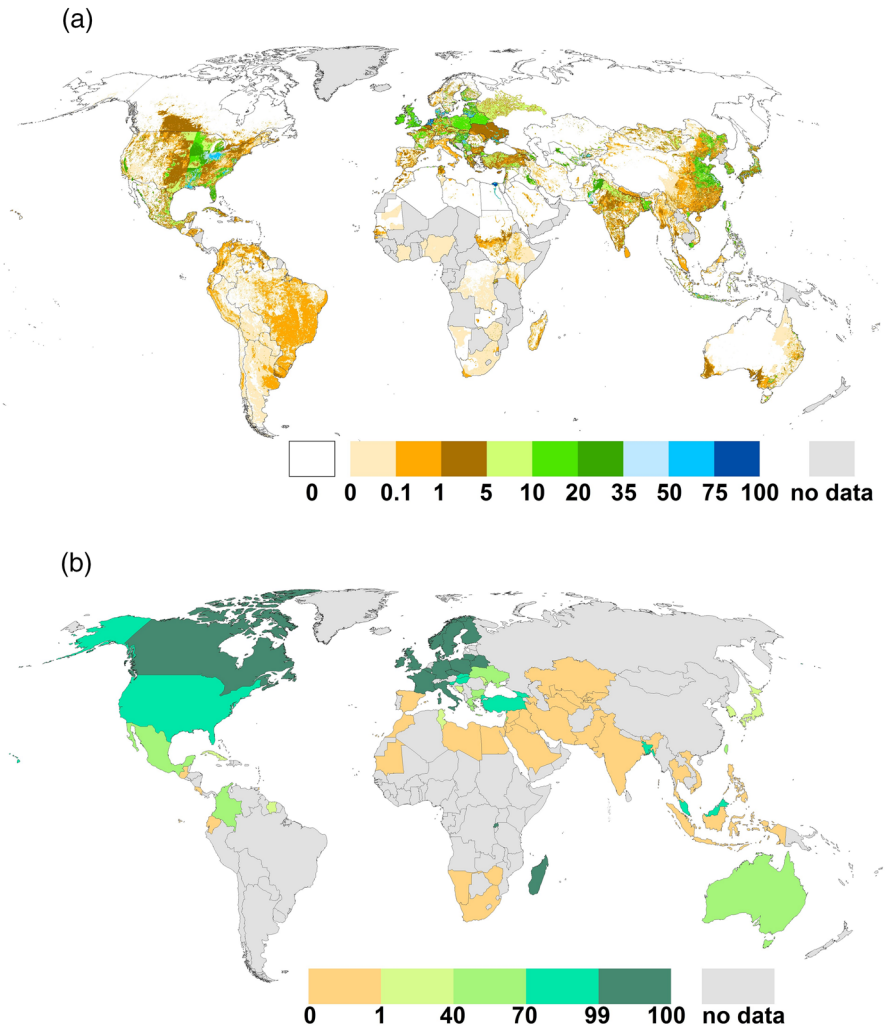

FIGURE A1 Percentage of 0.5° × 0.5° grid cell area with artificial drainage (Feick et al., 2005; a) and drained rainfed agricultural area as a fraction of total drained agricultural area per country (Feick et al., 2005; b)